IEEE Transactions on Nuclear Science, Vol.NS-25, No.4, August 1978

DIGITAL SIMULATION OF A COMMERCIAL SCALE HIGH TEMPERATURE GAS-COOLED REACTOR (HTGR) STEAM POWER PLANT

Asok Ray[+] and H. Frederick Bowman[*]

ABSTRACT

A nonlinear dynamic model of a commercial scale high temperature gas-cooled reactor (HTGR) steam power plant was derived in state-space form from fundamental principles. The plant model is 40th order, time-invariant, deterministic and continuous-time. Numerical results were obtained by digital simulation.

Steady-state performance of the nonlinear model was verified with plant heat balance data at 100, 75 and 50 percent load levels. Local stability, controllability and observability were examined in this range using standard linear algorithms. Transfer function matrices for the linearized models were also obtained. Transient response characteristics of 6 system variables for independent step disturbances in 2 different input variables are presented as typical results.

Simulation of the HTGR steam power plant provides the basis for (a) understanding the complex and highly interactive process dynamics, (b) designing an interactive multivariable controller, and (c) studying plant dynamic performance under various operating and upset conditions.

Modeling and simulation techniques developed in the work from which this paper is abstracted have general applicability, and can be readily adapted to the study of gas-cooled steam power plants.

INTRODUCTION

Existing commercial scale nuclear power plants are of the pressurized water reactor (PWR) and boiling water reactor (BWR) types. These plants have lower thermal efficiencies (~30 percent) in comparision to fossil-fueled plants because of reduced main steam temperatures. This deficiency is a motivation for high temperature gas-cooled reactor (HTGR) plants, in which steam conditions (2400 psig, 950/1000°F) are comparable to those in large fossil-fueled plants, resulting in improved thermal efficiency (~40 percent). Furthermore, HTGR plants have anticipated superior environmental and safety standards.[1,2]

Commercial scale HTGR plants have not yet been built; however, results from a pilot plant (Peach Bottom 1) are very encouraging.[3] Nevertheless, the control problems associated with HTGR plants are complex because the process is nonlinear with respect to operating load and it must be regulated by an interactive multivariable control system. A priori analytical studies are essential for design and development of commercial scale HTGR plants. This cannot be accomplished by simple extrapolation of pilot plant critical design parameters; more advanced analytical techniques are required. Mathematical modeling and simulation have proved to be useful analytical tools for investigation of potential operational and control problems in complex, multivariable systems, and for an appropriate controller design.[4]

Manuscript received: May 23, 1977;
Revised: February 8, 1978

+Technical Staff Member, The MITRE Corporation, Bedford, Mass.
*Associate Professor of Mechanical Engineering, Northeastern University, Boston, Mass.

This paper presents the philosophy and results of a nonlinear dynamic model formulated for digital simulation of an 1160 mw(e) HTGR steam power plant, formerly scheduled to be built at the Fulton Station of the Philadelphia Electric Company.[4,5] Simulation provides the basis for (a) understanding the complex and highly interactive process dynamics, (b) designing an interactive multivariable controller, and (c) studying overall system dynamic performance under various operating and upset conditions. Although specifically related to a particular HTGR plant, the modeling and simulation techniques reported in this paper have more general applicability, and can be readily adapted to the study of other gas-cooled steam power plants.

HTGR systems have been under development in the USA by the General Atomic Company for approximately 20 years. The first HTGR steam power plant - the 40 mw(e) pilot plant at Peach Bottom[3] was put into operation in 1967. A 330 mw(e) HTGR demonstration plant[6] is in the power escalation stage at Fort St. Vrain near Denver, Colorado. Commercial scale plants in the 770 mw(e) and 1160 mw(e) range have been under development, and feasibility studies suggest that a 1540 mw(e) capacity plant would be economical.[7] Recently, cost escalation and other program difficulties have resulted in deferral of the HTGR projects.[8]

SYSTEM DESCRIPTION

The commercial scale High Temperature Gas-cooled Reactor (HTGR) steam power plant consists of (a)nuclear steam supply (NSS) and (b) balance of plant (BOP) systems. The NSS and BOP equipment are located in different buildings, connected by water/steam (secondary coolant) paths as shown schematically in Figure 1 (see nomenclature for symbol description). A detailed plant and (proposed) control system schematic of a typical commercial HTGR steam plant is available in references (4,5).

The NSS system consists of a 3000 Mw thermal reactor, six once-through steam generators and six turbine-driven, variable-speed circulating compressors. The complete NSS system is enclosed within a pressurized concrete reactor vessel (PCRV).

The nuclear reactor is graphite-moderated, helium-cooled and fueled with coated microspheres of thorium

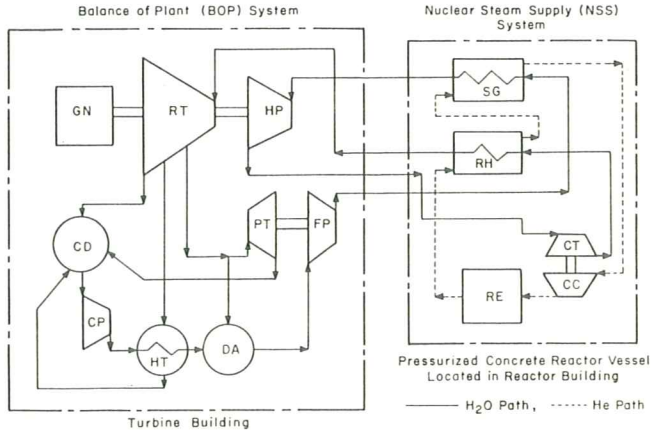

FIG. 1 OPERATIONAL SCHEMATIC OF HTGR STEAM POWER PLANT

0018-9499/78/0800-1068$00.75

and fully enriched (93%) uranium embedded in a carbonaceous binder. Reactor power level is regulated by positioning a control rod pair inside the core.

Forced circulation of helium (primary coolant) through the coolant channels in the reactor core is accomplished by six identical circulating compressors which discharge into a common plenum, located above the core. Each circulator compressor is of single-stage, axial-flow type and is driven by a single-stage, impulse turbine powered by high pressure turbine exhaust steam. Pressure ratio across the circulator turbine is maintained by positioning the bypass valve which acts as a shunting device. The circulator turbine-compressor speed is regulated by the turbine control valve.

The six steam generators are of once-through type and each unit consists of a reheater and a(subcritical) main steam generator. They can be considered as shell and tube heat exchangers having helium (primary coolant) on the shell side and water/steam (secondary coolant) on the tube side. Six reheaters receive cold (superheated) steam from the respective circulator turbine exhaust and discharge steam into the hot reheat header which feeds a pair of intermediate pressure turbines. Helium from a reheater passes through a duct to the respective main steam generator where feedwater is converted to superheated steam. Cold helium leaving a main steam generator flows to the respective circulator compressor through another duct. Six main steam generators discharge into the main steam header which feeds a pair of high pressure turbines.

The BOP system consists of two identical sets of equipment symmetrically connected by the feedwater, main steam, cold reheat, and hot reheat headers. Each set consists of a turbo-generator, condenser, feedwater heater train, and feedwater pumps, all located in the turbine building.

Each set of 580 Mw(e), 3600 rpm turbo-generator consists of a high pressure, an intermediate pressure and two low pressure turbines, and a synchronous generator, all mounted on the same shaft. The turbines are double-flow units of conventional reheat type, except that high pressure turbine exhaust steam is used to drive the helium circulator turbines before being reheated and returned to the intermediate pressure turbines.

Plant electrical power is regulated by positioning the governor valves with the aid of a digital electro-hydraulic (DEH) control system.[9] The DEH valve management program[10] is essentially a feedforward arrangement that incorporates dynamic characterization of the governor valves (with plant load demand as program input). The program provides either full arc (FA) or partial arc (PA) steam admission, and is capable of smooth transfer from one mode to the other.

The feedwater heater train consists of a gland steam heater, a drain cooler, three consecutive low pressure heaters, and a direct-contact deaerator which is the last heater in the train. The deaerator also serves as a feedwater reservoir. The feedwater pumping subsystem consists of two cascaded (and mechanically coupled) multi-stage centrifugal pumps driven by a variable-speed auxiliary turbine which receives extraction steam from the intermediate pressure turbine and discharges into the condenser. The feedwater pumps associated with each turbine discharge to a common feedwater header providing water for the six main steam generators.

To formulate a plant model for normal operating conditions, a simplified schematic was developed as shown in Figure 2 from a detailed diagram of HTGR steam power generation system[4,5,11] (see nomenclature).

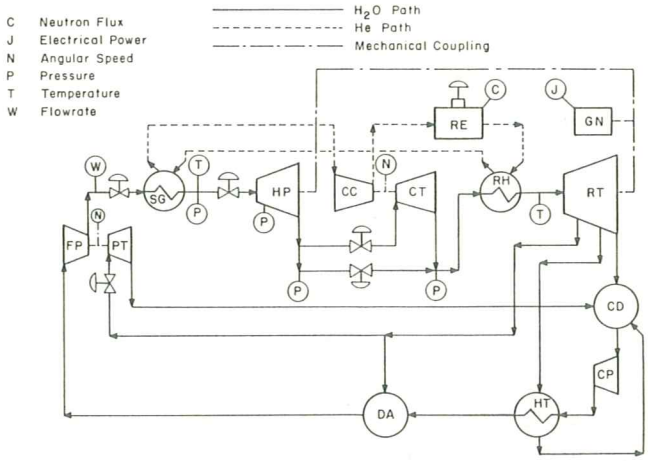

FIG. 2 SCHEMATIC OF MODELLED HTGR STEAM POWER PLANT

MODELING APPROACH

The physical process consists of distributed parameter dynamic elements, represented by a set of nonlinear partial differential equations with space and time as independent variables. Such systems are infinite-dimensional.[12] To obtain a numerical solution by digital computer, a finite-dimensional state-space model must be formulated. The partial differential equations were approximated via spatial discretization by a finite set of ordinary differential equations with time as the independent variable.[13] This approach has been shown to be adequate in the simulation of other power generation systems by experimental verification.[14,15]

Steady-state solutions of the nonlinear dynamic model were obtained at different points in the operating range. The model was linearized at these steady-state conditions and system eigenvalues were evaluated. In some cases, model structure reformulation was necessary for efficient numerical solution (for example, very large negative eigenvalues are not desirable).

To organize the model equations, a solution diagram[4,5,11] was developed as shown in Figure 3 (see nomenclature). Each block in the diagram represents a physical component or a group of components. The lines interconnecting the blocks indicate the direction of information flow or "model causality". The diagram shows how the individual component models

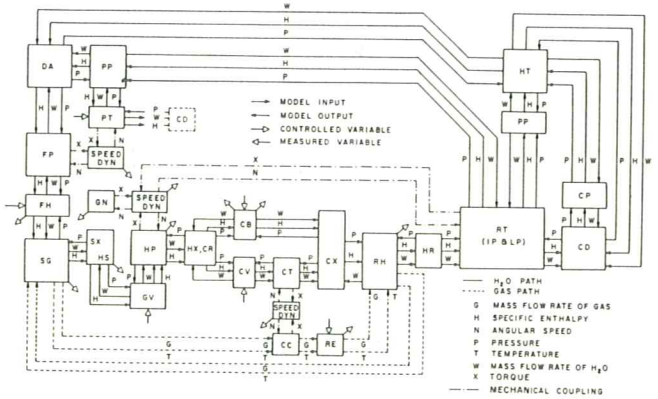

FIG. 3 MODEL SOLUTION DIAGRAM

mathematically interface with each other and ensures consistent causality for the complete set of equations defining the physical system. Following the development of the solution diagram, the task of plant modeling was accomplished in two steps: first, modeling of individual components or groups of components; and second, formulation of an overall plant model by appropriate interconnection of the individual component models.

Step 1 included determination of steady-state solutions and eigenvalues of individual components at various operating points. The steady-state model results were verified with design data, and the eigenvalues were examined for frequency range. Step 2 incorporated sequential interconnection of component models according to the model solution diagram (Figure 3). In this process, the steady-state solutions and eigenvalue sets of the augmented models were examined at each phase of interconnection. Due to the interactive nature of the process, certain eigenvalue sets of the augmented models were found to be significantly different from those of the component models that constitute the augmented model.

In addition to steady-state evaluation and eigenvalue determination the family of linearized models (at different operating points) were tested for controllability and observability. The set of controllable and observable state-variable structures of the plant allows design of the multivariable controller in the time domain. To perform a frequency domain design, a family of transfer function matrices were generated.

PLANT MODEL

The equations used to formulate the plant model were: (1) Fundamental equations of mass, momentum, and energy conservation; (2) Semi-empirical relationships for fluid flow and heat transfer; (3) Neutron kinetic equations; and (4) State relations for thermodynamic properties of the working fluids. Appropriate functional forms of the above equations are given in earlier publications.[11,16,17]

The primary assumption in this study was that the infinite-dimensional distributed parameter process can be represented by a finite-dimensional lumped parameter model through appropriate selection of control volumes.[13,14,15] Additional assumptions were: (1) Uniform fluid flow across any cross-section; (2) Negligible axial heat transfer in primary coolant, secondary coolant, tube wall, and reactor core; (3) Perfect thermal insulation between plant components and the environment; (4) Negligible transfer of stored thermal energy from insulated pipelines, ducts, turbine blades, etc. during thermal transients of the working fluids; (5) Negligible compressibility and flow inertia of the primary coolant; and (6) Negligible pressure drop due to velocity and gravitational heads in the primary coolant and steam path.

The plant model was developed for normal operating conditions from the simplified schematic in Figure 2. Development of model equations and the basis for state variable selection are available in reference(11); they are not repeated here due to sheer bulk. However, a brief discussion on the nuclear reactor model is given in Appendix I; and the state $\underset{\sim}{x}$, output $\underset{\sim}{y}$, and input (control) $\underset{\sim}{u}$ variables are listed in Appendix II.

Utilizing the model solution diagram, the system was partitioned into six subsystems to arrive at the overall plant model. The six subsystems are: nuclear reactor, helium circulation; steam generators; turbogenerators and steam headers; condenser and feedwater heater; and feedwater pumps and headers. The system parameters used in the model were calculated from steady-state system design data. The numerical algorithms used in simulation and the basis for their selection are presented and discussed in reference (11).

The nonlinear model was simulated on an IBM 370/158 digital computer in CSMP-III[18] for obtaining the (open loop) plant transients. For model linearization and subsequent mathematical operations, a FORTRAN-IV version of the CSMP-III code was used as a subroutine in a general purpose analytical program.[19] Load modules were created where the system parameters, disturbance signals and initial values of the state variables were input data. Using this load module typical computer execution time (on an IBM 370/158 machine) was about 80 C.P.U. seconds for simulating plant transients for an 800 second period. Core size requirement was 120K bytes (1 byte=8 bits).

COMPARISON WITH EXISTING MODELS

In this section, the major differences between earlier work in HTGR steam power plant modeling and the present analysis are noted. However, modeling variations do exist due to different configurations in the physical plants; thus, the modeling techniques only are discussed here.

In the work reported here, the most important modeling decisions appear in the selection of state variables so that the more critical plant components are modeled in greater detail (for example, the main steam generator was modeled with eight state variables, whereas the complete condenser and the feedwater heating subsystem model has only two state variables).[11] Further, the nonlinear process has been modeled over an operating range of interest.

Hastings et al. presented a digital simulation of the 330 mw(e) Fort St. Vrain HTGR plant.[20] The plant model was primarily used for obtaining system transients for various disturbance signals. The development of model equations, selection of state variables, and modeling considerations were neither presented nor referenced. A simple controller was incorporated in the system model. Though need for better controller design was recognized, the plant model apparently was not tested for stability, controllability, and observability. No significant control or operational problems were reported.

Richardson outlined a first-principle model of a 3000mw(t) HTGR plant at 100 percent load.[21] The plant model was recommended for controller design in the frequency domain. The nuclear steam supply system (NSSS) was emphasized in the model. Fundamental equations of fluid flow were oversimplified, and steam properties were approximated by perfect gas laws. The number of state variables, basis for their selection, and causality for component model interconnection were not clearly indicated. The model performance for lower load was not evaluated and thus variations in system eigenvalues with plant load could not be determined. Further, the plant model was not tested for controllability and observability. Although this study is an important advancement in HTGR system modeling and simulation, it is not suitable for representing the nonlinear system over a wide operating range. Control systems designed on the basis of a linearized model at full load may not be adequate at lower loads.

Bogrinski et al. described the plant model and controller design for a thorium high temperature reactor (THTR) steam power generation system.[22] Although a high order nonlinear plant model was formulated, the control system apparently was designed by trial and error using

oversimplified transfer functions. The basis for selection of state variables and model evaluation at different load levels (i.e., steady-state solutions at different load levels, variations of system eigenvalues with plant load, etc.) were not presented.

Recently, McNamara et al. presented the results of the Fort St. Vrain circulator auxiliaries system simulation.[23] The simulation results were compared with experimental test data to establish model validity. However, the control system was apparently not designed through a systematic analytical approach. Although the model represents only a part of the HTGR system, it contains 83 differential equations. The entire system model is expected to be even larger and analytical interactive controller design is difficult unless the model order is reduced. This work shows that the fluid system in HTGR steam plants can be represented by a lumped parameter model.

MODEL RESULTS

The simulation results are presented and the plant model is evaluated as follows:

Steady-state Solution and Linearization

Steady-state solutions of the nonlinear model were obtained at several operating points in the load range of 100 to 25 percent. Available steady-state heat balance data at 100, 75 and 50 percent load agree closely with the corresponding model results as is evident in Table 1. This agreement established partial validity of the model in the load range of 100 to 50 percent. Complete model validation can only be obtained by comparison with steady-state and transient field data (which are not available). Below 50 percent load, model results could not be verified due to lack of heat balance data. Generally, nuclear power plants are not required to operate below 50 percent load; thus, the model is capable of simulating the real plant in the normal operating conditions. The model can also be used in the event of severe upset conditions, but may suffer some loss of precision. For example, in a reactor scram, the system maintains 15 percent steam flow to remove decay heat from the reactor core. Even in such a case, it is helpful to use the model to understand the processes that will occur.

The nonlinear plant model was linearized at several steady-state operating points in the following form:

$$\dot{\delta x} = A\,\delta x + B\delta u$$

$$\delta y = C\,\delta x + D\delta u$$

The matrices A, B, C, and D for the linearized models are not presented here due to sheer bulk.

System Eigenvalues

A family of linearized models at a number of operating points approximates the global characteristics of the nonlinear process in the operating range. System stability and selection of numerical integration method were determined by the location and range of the system eigenvalues (i.e., eigenvalues of the A-matrix). Table 2 shows the system eigenvalues at 100, 75 and 50 percent load. Examination of the smallest (magnitude) eigenvalues in Table 2 shows that the (open loop) plant stability deteriorates

TABLE 1
COMPARISON OF STEADY-STATE MODEL RESULTS WITH DESIGN DATA

Description	100% Load		75% Load		50% Load	
	Model Results	Heat Balance Data	Model Results	Heat Balance Data	Model Results	Heat Balance Data
Helium mass flowrate lbm/sec	5.174e+02	5.177e+02	4.108e+02	4.084e+02	2.920e+02	2.914e+02
Helium temperature at compressor inlet F	5.902e+02	5.900e+02	5.616e+02	5.580e+02	5.288e+02	5.280e+02
Helium temperature at reactor outlet F	1.333e+03	1.340e+03	1.275e+03	1.290e+03	1.214e+03	1.223e+03
Electrical generator output power MW	5.885e+02	5.800e+02	4.412e+02	4.350e+02	2.913e+02	2.900e+02
Normalized neutron flux pu	9.853e-01	9.800e-01	7.581e-01	7.607e-01	5.216e-01	5.200e-01
Feedwater mass flowrate lbm/sec	1.109e+03	1.116e+03	8.321e+02	8.368e+02	5.547e+02	5.564e+02
Feed pump pressure psia	3.195e+03	3.197e+03	2.854e+03	2.863e+03	2.608e+03	2.615e+03
Main steam pressure psia	2.415e+03	2.415e+03	2.415e+03	2.415e+03	2.415e+03	2.415e+03
Main steam temperature F	9.500e+02	9.500e+02	9.500e+02	9.500e+02	9.500e+02	9.500e+02
HP turbine impulse stage pressure psia	1.748e+03	1.750e+03	1.285e+03	1.290e+03	8.322e+02	8.400e+02
HP turbine exhaust pressure psia	9.553e+02	9.580e+02	7.176e+02	7.190e+02	4.786e+02	4.790e+02
HP turbine exhaust enthalpy BTU/lbm	1.335e+03	1.335e+03	1.330e+03	1.325e+02	1.321e+03	1.321e+03
Circulator turbine bypass valve inlet pressure psia	9.373e+02	9.400e+02	7.042e+02	7.060e+02	4.698e+02	4.700e+02
Circulator turbine inlet pressure psia	9.069e+02	9.020e+02	6.165e+02	6.190e+02	3.948e+02	3.940e+02
Circulator turbine exhaust pressure psia	6.509e+02	6.510e+02	4.890e+02	4.830e+02	3.263e+02	3.250e+02
Circulator turbine exhaust enthalpy BTU/lbm	1.308e+03	1.306e+03	1.313e+03	1.308e+03	1.312e+03	1.310e+03
Mass flowrate through circulator turbine lbm/sec	3.559e+02	3.527e+02	2.208e+02	2.234e+02	1.336e+02	1.307e+02
Mass flowrate through turbine bypass valve lbm/sec	1.263e+01	1.590e+01	5.562e+01	5.264e+01	5.063e+01	5.269e+01
Hot reheat steam pressure psia	5.500e+02	5.500e+02	4.128e+02	4.140e+02	2.753e+02	2.760e+02
Hot reheat steam temperature F	1.000e+03	1.000e+03	1.000e+03	1.000e+03	1.000e+03	1.000e+03
Mass flowrate through IP turbine lbm/sec	1.106e+03	1.089e+03	8.292e+02	8.170e+02	5.528e+02	5.544e+02
IP turbine exhaust pressure psia	1.701e+02	1.700e+02	1.286e+02	1.280e+02	8.597e+01	8.580e+01
IP turbine exhaust enthalpy BTU/lbm	1.376e+03	1.376e+03	1.380e+03	1.381e+03	1.386e+03	1.386e+03
LP turbine extraction pressure psia	8.167e+01	8.160e+01	6.217e+01	6.300e+01	4.186e+01	4.150e+01
LP turbine extraction enthalpy BTU/lbm	1.216e+03	1.216e+03	1.222e+03	1.221e+03	1.231e+03	1.230e+03
LP turbine exhaust enthalpy BTU/lbm	1.032e+03	1.035e+03	1.050e+03	1.047e+03	1.076e+03	1.073e+03
Condenser pressure psia	1.125e+00	1.125e+00	1.125e+00	1.125e+00	1.125e+00	1.125e+00
Steam flowrate to lumped heater lbm/sec	1.839e+02	1.845e+02	1.246e+02	1.260e+02	7.127e+01	7.123e+01
Tube water temperature at heater exit F	3.031e+02	3.030e+02	2.847e+02	2.850e+02	2.602e+02	2.600e+02
Heater shell pressure psia	7.532e+01	7.500e+01	5.837e+01	5.800e+01	4.004e+01	4.000e+01
Deaerator water temperature F	3.627e+02	3.630e+02	3.419e+02	3.410e+02	3.141e+02	3.140e+02
Deaerator steam inlet mass flowrate lbm/sec	5.852e+01	5.850e+01	4.059e+01	4.100e+01	2.437e+01	2.450e+01
Feed pump turbine steam mass flowrate lbm/sec	4.484e+01	4.500e+01	3.291e+01	3.280e+01	2.416e+01	2.400e+01
Feed pump turbine exhaust enthalpy BTU/lbm	1.079e+03	1.076e+03	1.103e+03	1.100e+03	1.131e+03	1.130e+03

TABLE 2

SYSTEM EIGENVALUES (IN SEC^{-1}) AT 100, 75 AND 50 PERCENT RATED PLANT LOAD

100 Percent Load		75 Percent Load		50 Percent Load	
REAL PART	IMAGINARY PART	REAL PART	IMAGINARY PART	REAL PART	IMAGINARY PART
-0.571171D-02	0.0	-0.150080D-03	0.0	0.332617D-02	0.0
-0.112388D-01	0.0	-0.831845D-02	0.0	-0.527398D-02	0.0
-0.196218D-01	0.0	-0.162759D-01	0.0	-0.179990D-01	0.212385D-02
-0.285753D-01	0.541951D-02	-0.237066D-01	0.362761D-02	-0.179990D-01	-0.212385D-02
-0.285753D-01	-0.541951D-02	-0.237066D-01	-0.362761D-02	-0.117566D-01	0.0
-0.228731D-01	0.115335D-01	-0.187558D-01	0.135153D-01	-0.138191D-01	0.135920D-01
-0.228731D-01	-0.115335D-01	-0.187558D-01	-0.135153D-01	-0.138191D-01	-0.135920D-01
-0.761739D-01	0.704641D-01	-0.655440D-01	0.617613D-01	-0.554580D-01	0.454828D-01
-0.761739D-01	-0.704641D-01	-0.655440D-01	-0.617613D-01	-0.554580D-01	-0.454828D-01
-0.177607D+00	0.0	-0.177992D+00	0.0	-0.125837D+00	0.896058D-01
-0.298011D+00	0.0	-0.153525D+00	0.130007D+00	-0.125837D+00	-0.896058D-01
-0.367089D+00	0.0	-0.153525D+00	-0.130007D+00	-0.165317D+00	0.0
-0.172259D+00	0.165940D+00	-0.303131D+00	0.0	-0.242484D+00	0.0
-0.172259D+00	-0.165940D+00	-0.277481D+00	0.0	-0.287062D+00	0.513505D-02
-0.327842D+00	0.198199D+00	-0.363486D+00	0.0	-0.287062D+00	-0.513505D-02
-0.327842D+00	-0.198199D+00	-0.319853D+00	0.167507D+00	-0.285609D+00	0.128243D+00
-0.477764D+00	0.0	-0.319853D+00	-0.167507D+00	-0.285609D+00	-0.128243D+00
-0.593445D+00	0.973000D-01	-0.522385D+00	0.0	-0.456100D+00	0.0
-0.593445D+00	-0.973000D-01	-0.469556D+00	0.0	-0.452885D+00	0.0
-0.793191D+00	0.748895D-01	-0.650709D+00	0.0	-0.503246D+00	0.0
-0.793191D+00	-0.748895D-01	-0.680028D+00	0.0	-0.640094D+00	0.0
-0.840314D+00	0.0	-0.681863D+00	0.106345D+00	-0.584937D+00	0.0
-0.111869D+01	0.0	-0.681863D+00	-0.106345D+00	-0.112579D+01	0.0
-0.961715D+00	0.0	-0.120442D+01	0.0	-0.961209D+00	0.0
-0.208092D+01	0.0	-0.961525D+00	0.0	-0.150649D+01	0.0
-0.163734D+01	0.0	-0.166549D+01	0.0	-0.125079D+01	0.0
-0.209768D+01	0.0	-0.185546D+01	0.0	-0.158961D+01	0.636161D-01
-0.234956D+01	0.0	-0.191856D+01	0.0	-0.158961D+01	-0.636161D-01
-0.247690D+01	0.0	-0.181325D+01	0.0	-0.158352D+01	0.0
-0.242819D+01	0.0	-0.214220D+01	0.0	-0.252893D+01	0.0
-0.362567D+01	0.0	-0.269495D+01	0.0	-0.232700D+01	0.0
-0.437588D+01	0.0	-0.247246D+01	0.0	-0.306582D+01	0.960668D+00
-0.528814D+01	0.531959D+00	-0.429274D+01	0.0	-0.306582D+01	-0.960668D+00
-0.528814D+01	-0.531959D+00	-0.388179D+01	0.0	-0.343473D+01	0.316311D+00
-0.648928D+01	0.0	-0.467946D+01	0.0	-0.343473D+01	-0.316311D+00
-0.643099D+01	0.0	-0.877092D+01	0.0	-0.451334D+01	0.0
-0.958855D+01	0.0	-0.112412D+02	0.0	-0.106099D+02	0.0
-0.938333D+01	0.0	-0.989858D+01	0.0	-0.123786D+02	0.0
-0.166167D+02	0.0	-0.127937D+02	0.0	-0.113789D+02	0.0
-0.123327D+02	0.0	-0.114419D+02	0.0	-0.218733D+02	

monotomically with load. Further, significant variations of some of the eigenvalues at different load levels demonstrate the nonlinear plant characteristics.

The positive eigenvalue (at 50 percent load) was found to be significantly dependent on the state variables, steam density and specific enthalpy, at the main steam generator discharge. This led to a stability investigation of the main steam generator (SG) and its discharge node (SX) in Figure 3. All eigenvalues of these isolated components have negative real parts when constant inputs are assumed (as determined during formulation of component models). For example, the main steam generator model with constant discharge pressure as an input is stable at 50 percent load. However, when the two component models are interconnected either alone or with the rest of the plant, the situation changes due to inherent feedback.

This low load instability is thought to derive from the complex boiling heat transfer and flow-pressure drop characteristics in the two-phase region of the once-through subcritical steam generators.[24] Nevertheless, due to mutual coupling of process variables (such as temperature, flow, etc. of both primary and secondary coolants) in various plant components, it is difficult to establish a firm heuristic reason for plant instabilities. It is felt that stability can be improved by increasing fluid flow resistance in the water/steam path. Thus, a change in (main steam generator) inlet orifice design is likely to remove low load instability. However, for a controllable and observable system, low frequency instability in open loop is not a serious problem and can be overcome in closed loop by an appropriate controller. Since a controller designed solely on the basis of the high load plant model may yield unsatisfactory performance at low loads, attention must be paid to control system design in overcoming any potential instability at low loads.[25]

Local Controllability and Observability

Since sufficiency conditions for controllability and observability of nonlinear systems are difficult to obtain, these properties were tested locally on the linearized models. Initial results were as follows: controllability of 39 states (1 state being uncontrollable for all linearized models) and complete observability for all linearized models.

Lack of controllability for the linearized models was expected due to the nonlinear relationship between steam flow and governor valve area. Eight governor valves and associated impulse stage nozzles were modelled in two groups, namely wide open and partially open valves (see development of model equations in reference (11) for detail) to determine steam flow for sonic and compressible subsonic conditions. An electrical analog diagram for this arrangement is shown in Figure 4.

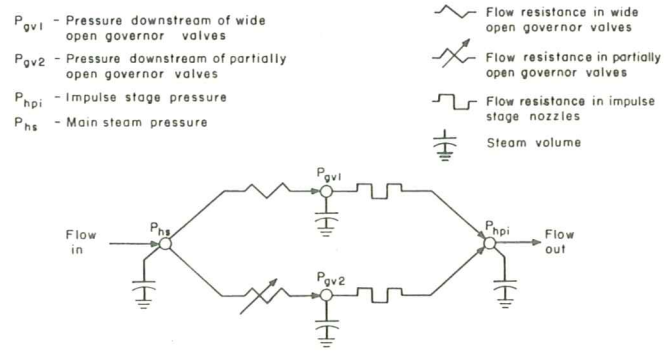

FIG. 4 ELECTRICAL ANALOG OF GOVERNOR VALVE ARRANGEMENT

Following a small perturbation in the governor valve area the flow resistance due to partially open governor valves is disturbed. Referring to Figure 4, the state P_{gv2} can thus be easily controlled but P_{gv1} is affected by changes in the states, P_{hs} and P_{hpi}. For testing purposes, the area due to wide open governor valves was made an additional input and the system was found to be completely controllable. This suggests that either the original linearized models are genuinely uncontrollable or the numerical algorithm[26] is not sufficiently accurate. Since the area of a wide open valve is really constant, and inappropriate as a control input, and since a better numerical method was not available, part of the linearized model structure was reformulated to obtain complete controllability.

In the reformulation process, the state variable P_{gv1} was eliminated by algebraically solving the linearized state equations for P_{gv1} (i.e., one of the system eigenvalues was pushed to negative infinity). In solving the nonlinear model equations, deletion of P_{gv1} generates an implicit loop which may fail to converge for certain sonic and subsonic flow conditions at the impulse stage nozzles. For the linearized models, the implicit loop reduces to a linear algebraic equation which is easily solved. Following this step, the linearized model order was reduced from 40 to 39 for each load level. The 39th order linearized models were found to be completely controllable and observable.

Eigenvalue ranges of the 39th order models were identical to those of the respective 40th order models, i.e. the smallest and largest (magnitude) eigenvalues were unchanged. In each case, a real negative eigenvalue of approximate magnitude 4.5 was eliminated and some other eigenvalues in the range of -1.0 to -7.0 were mildly affected.

The state variable P_{gv1}, which was eliminated to make the linear models controllable, must be retained in the nonlinear model for two reasons: determination of system transients following large disturbances (for example, turbine load rejection when number of wide open governors valves may change significantly) and determination of steady-state solutions of the model equations at different plant operating points.

Frequency Response

System transfer function matrices for the prescribed output and input (control) variables (see Appendix II) were obtained for the 39th order linearized models at different load levels. Using standard computational techniques[19], the magnitude and phase of transfer functions were numerically obtained for a wide range of discrete frequencies. Space limitations do not permit the transfer functions to be listed here, but they can be found in reference(11).

Transient Response of the Nonlinear Model

Dynamic response of the (open loop) nonlinear plant model can be obtained by perturbing input (control) variables as long as the model is stable in the range of operation. Transient response of the nonlinear HTGR plant model was obtained for independent step disturbances in the five input (control) variables from the equilibrium condition at 100 percent load. Since governor valves and reactor control rods regulate plant electrical power and thermal fission power, respectively, the transient responses due to independent disturbances in these two input variables only are presented here.

Transient responses of a number of system variables are given in Figures 5-10, where each figure shows the response of a particular system variable to a 5 percent step decrease in governor valve area, and to a 5 percent step increase in reactor control rod insertion (equivalent to an instantaneous reactivity change of -0.0012 unit $\simeq 0.25\beta$ where $\beta = 0.0047$ is total delayed neutron fraction). The step disturbances were applied at time t=40 seconds to display the steady-state condition (at 100 percent load in this case) before initiating the disturbances. Dynamic responses were observed for an 800 second period at 20 second intervals.

Figure 5 shows the neutron flux transients normalized with respect to the rated reactor capacity. For normal operation of the reactor, thermal fission power is directly proportional to neutron flux. Governor valve area reduction has no significant effect on neutron flux. A slight decrease does result from a higher reactor core temperature due to negative feedback of temperature-induced reactivity associated with the fuel. Higher core, helium and steam temperatures follow the reduction in steam flowrate. Reactor rod insertion, on the other hand, abruptly reduces neutron flux due to the rod-induced prompt neutron reactivity reduction. Subsequently, as core temperature decreases, the neutron flux partially recovers due to the negative temperature coefficient of reactivity. This temperature effect overwhelms that of the delayed neutron concentrations.

Feedwater flow dynamics are shown in Figure 6. A decrease in governor valve area increases secondary coolant flow resistance resulting in lower feedwater flow. Transients are primarily due to inertia of the feedwater path from the deaerator to the main steam generator, and moment of inertia of the feed pump rotor (feed pump speed strongly influences feedwater pressure). An increase in reactor rod insertion reduces thermal fission power resulting in lower hot reheat steam temperature. Thus, feed pump turbine power is reduced due to changes in intermediate pressure turbine extraction steam condition. Decreased reactor power reduces thermal energy transfer to the main steam generator where economizer length increases at the cost of superheater length[16,17] resulting in decreased flow resistance. In the steady-state, this reduction in steam generator flow resistance is almost compensated

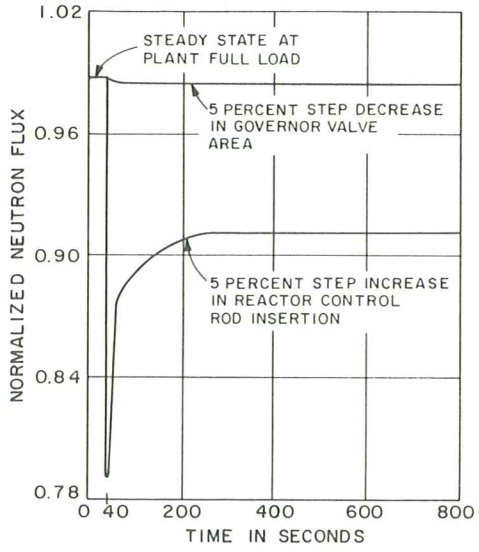

FIG. 5 NORMALIZED NEUTRON FLUX TRANSIENTS DUE TO STEP DISTURBANCES FROM FULL LOAD

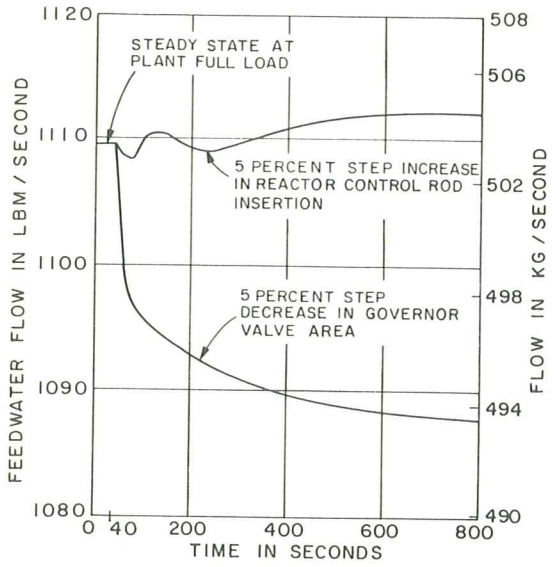

FIG. 6 FEEDWATER FLOW TRANSIENTS DUE TO STEP DISTURBANCES FROM FULL LOAD

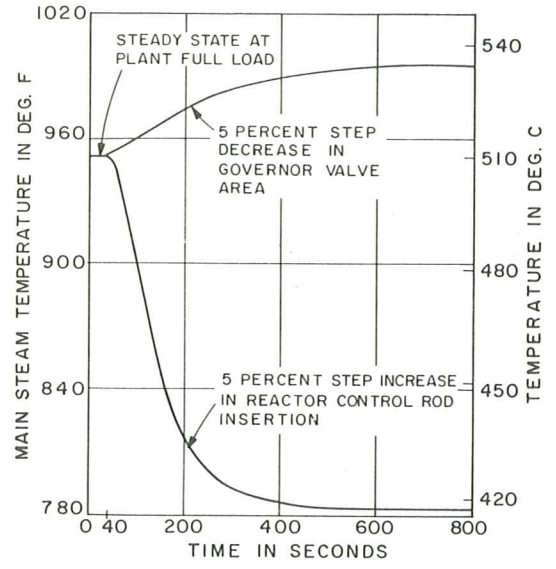

FIG. 7 MAIN STEAM TEMPERATURE TRANSIENTS DUE TO STEP DISTURBANCES FROM FULL LOAD

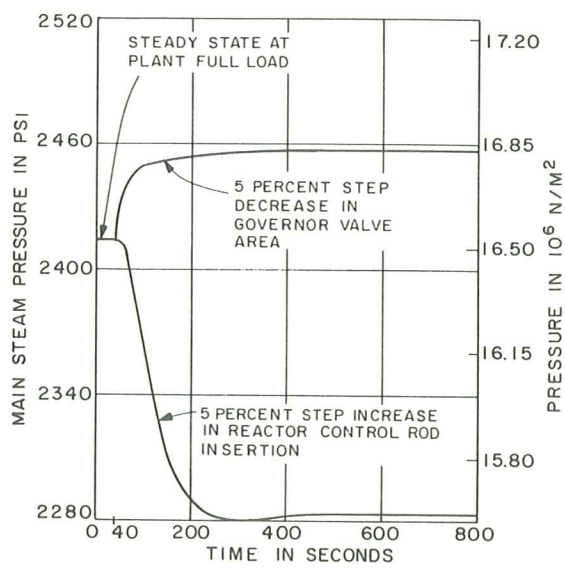

FIG. 8 MAIN STEAM PRESSURE TRANSIENTS DUE TO STEP DISTURBANCES FROM FULL LOAD

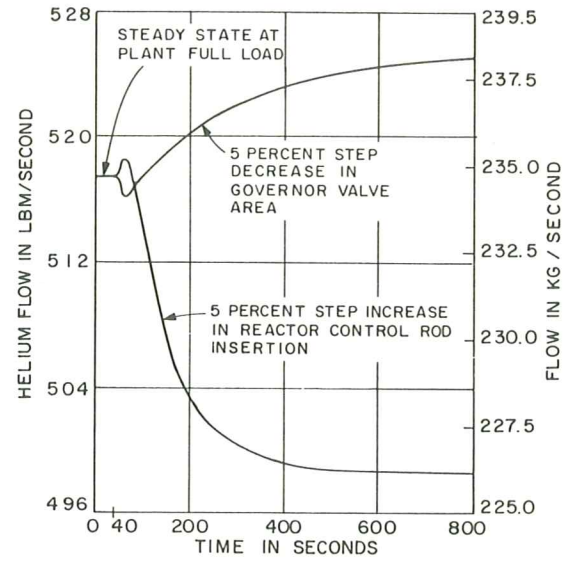

FIG. 9 HELIUM FLOW TRANSIENTS DUE TO STEP DISTURBANCES FROM FULL LOAD

for by feed pump pressure reduction (due to reduced feed pump speed), and only a slight increase in feedwater flow results. Initial oscillations in feedwater flow exhibit nonlinear flow characteristics of thermal-hydraulic coupling between the primary and secondary coolants.

Main steam temperature transients are shown in Figure 7. Following a governor valve area reduction, feedwater flow decreases whereas reactor power remains substantially constant (Figure 5). Main steam temperature increases because of a larger residence time of superheated steam in the main steam generator (due to longer superheater[16,17]). In contrast, reactor rod insertion causing lower thermal fission power reduces main steam temperature.

Figure 8 shows main steam pressure dynamics. Increased flow resistance due to governor valve area reduction produces a rise in upstream throttle steam pressure. This process is relatively fast due to dominating hydraulic transients. Reactor rod insertion produces lower feed pump pressure (due to a decrease in the pump power); thus, main steam pressure is reduced.

Helium flow dynamics are shown in Figure 9. Following a governor valve area reduction, helium flow initially dips due to a drop in high pressure turbine exhaust steam pressure, which feeds the helium circulating turbines. Later on, due to a rise in main steam temperature, enthalpy at circulator turbine inlet increases. A decrease in steam flow is overcompensated by an increase in enthalpy differential across the circulator turbine. Thus, circulator turbine is provided with augmented power increasing its speed and helium flow. With a reactor rod insertion, helium flow initially rises due to lower reheater steam pressure (i.e., circulator turbine exhaust pressure) resulting from reduced reactor power. Later on, as the main steam temperature decreases, steam power input to the circulator turbine reduces, and helium flow relaxes to a lower steady-state value.

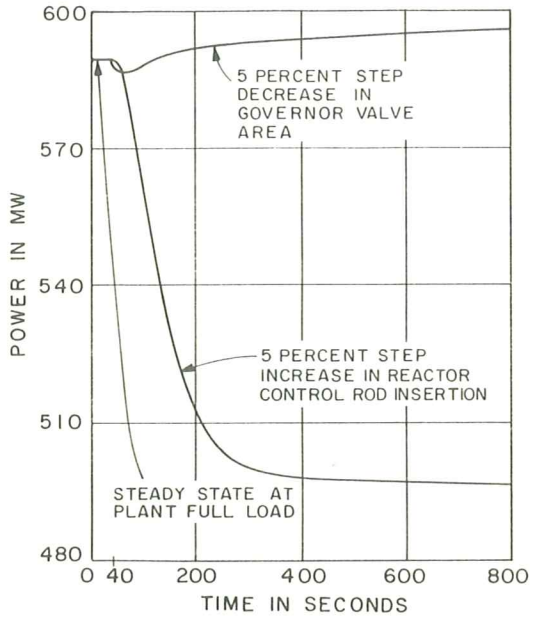

FIG. 10 ELECTRICAL POWER TRANSIENTS DUE TO STEP DISTURBANCES FROM FULL LOAD

Electrical power transients are shown in Figure 10. A decrease in governor valve area initially reduces electrical power due to a drop in high pressure turbine power. Within several minutes, the electrical power exceeds its original value due to improved thermal efficiency resulting from increased steam temperatures. Also, in this case, a decrease in steam flow is overcompensated by increments in enthalpy differentials across the main steam turbines. On the other hand, with increased reactor rod insertion, electrical power decreases due to reduced thermal fission and lower thermal efficiency resulting from lower steam temperatures.

CONCLUSIONS AND MODEL UTILIZATION

Typical simulation results and dynamic modeling techniques for a commercial scale high temperature gas-cooled reactor (HTGR) steam power generation system have been presented. This 40th order, nonlinear, time-invariant, deterministic, and continuous-time model was formulated in state-space from fundamental principles, and numerical results were obtained by digital simulation.

The results are useful for understanding complex and highly interactive process dynamics and also as a predictor of potential operational and control problems of large-scale HTGR steam power plants.

In addition to controller design and evaluation, the basic model structure formulated here can be extended to investigate the following: plant start-up and shut-down (normal and emergency) and plant parameter sensitivity analyses (i.e., influence of heat transfer, fluid mechanic, and thermodynamic relationships on system performance).

NOMENCLATURE FOR FIGURES

CB	Helium Circulator Turbine Bybass Valve
CC	Helium Circulator Compressor
CD	Condenser
CP	Condensate Pump
CR	Cold Reheat Header
CT	Helium Circulator Turbine
CV	Helium Circulator Turbine Steam Admission Valve
CX	Helium Circulator Turbine Exhaust
DA	Daerator
FH	Feedwater Header including Trim Valve
FP	Feedwater Pump
GN	Electrical Generator
GV	High Pressure Turbine Governor Valves
HP	High Pressure Turbine
HR	Hot Reheat Header
HS	Main Steam Header
HT	Low Pressure Heater
HX	High Pressure Turbine Exhaust
IP	Intermediate Pressure Turbine
LP	Low Pressure Turbine
PP	Pipe Line with a Check Valve
PT	Feedwater Pump Turbine
RE	Nuclear Reactor
RH	Reheat Steam Generator
RT	Reheat Turbine (1 Intermediate and 2 Low Pressure Turbines)
SG	Main Steam Generator
SX	Main Steam Generator Discharge

ACKNOWLEDGEMENTS

The authors acknowledge the benefits of discussions with Dr. D.A. Berkowitz, Dr. J.P. McDonald, Ms. N.E. Pettengill and Mr. J.A. Rovnak.

REFERENCES

1. P. Fortesque and H.B. Stewart, "The Role of HTGR's and FBR's in Meeting the Energy Crisis," ASME Winter Annual Meeting, New York, Nov. 1972.
2. G.J. Malek and R.S. Scheicher, "Design Bases for HTGR Core Cooling Systems," ASME Winter Annual Meeting, Detroit, Mich., Nov. 1973.
3. T.G. Dunning, "Design and Operational Experience with Control Instrumentation Systems, Peach Bottom Atomic Power Station Unit 1," IEEE Trans. Nuc. Sci., Vol. NS-19, No. 1, pp 843-845, Feb. 1972.
4. D.A. Berkowitz, Ed., Proceedings of the Seminar on Boiler Modeling, The MITRE Corporation, Bedford, Mass., Nov. 1974.
5. W.T.F. Broer, K.O. Jaegtners, J.P. McDonald, and R.W. McNamara, "Fulton Station Plant Dynamic Simulation," Joint IEEE/ASME Power Generation Technical Conference, Miami Beach, Flordia, Sept. 15-19, 1974.
6. R.E. Walker and T.A. Johnston, "Fort St. Vrain Nuclear Power Station," Nuc. Eng. Int., Vol. 14, No. 163, pp. 1069-1073, Dec. 1969.
7. E. Oakes, "Gas-cooled Reactors-Availability, Reliability and Efficiency," Proceedings of the workshop on Increasing Efficiency and Effectiveness in Electric Power Generation, The MITRE Corporation, McLean, Va., Report No. MTR-7032, pp 237-260, Feb. 1976.
8. Nuclear News, Vol. 18, No. 13, pp 21-22, Oct. 1975.
9. L.B. Podolsky, R.L. Osborne and R.S. Heiser, "Digital Electrohydraulic Control for Large Steam Turbines," Proceedings of the International ISA Symposium, New York, May, 1971.
10. L.B. Podolsky and V.G. Ronnen, "Valve Management - A Feedforward System for Digital Electro-hydraulic Turbine Control," Proceedings of the International ISA Symposium, Oct. 1973.

11. A. Ray, "Mathematical Modeling and Digital Simulation of Commercial Scale High Temperature Gas-Cooled Reactor (HTGR) Steam Power Plant." Ph.D. thesis, Department of Mechanical Engineering, Northeastern University, Boston, Mass., June 1976.
12. J.E. Rubio, The Theory of Linear Systems, Academic Press, New York, 1971.
13. M.P. Polis and R.E. Goodson, "Parameter Identification in Distributed Systems: A Synthesizing Overview," Proceedings of the IEEE, Vol. 64, No.1, pp. 45-61, Jan. 1976.
14. J. Adams, D.R. Clark, J.R. Louis, and J.P. Spanbauer, "Mathematical Modeling of Once-through Boiler Dynamics," IEEE Trans. PAS, Vol. PAS-84, No. 2, pp. 146-156, Feb. 1965.
15. H.G. Kwatny, J.P. McDonald, J.H. Spare, "A Nonlinear Model for Reheat Boiler-Turbine-Generator Systems: Part II - Development," Preprints, Joint Automatic Control Conference, pp. 227-236, 1971.
16. A. Ray, "A Nonlinear Dynamic Model of a Once-through Subcritical Steam Generator," Mechanical Engineer thesis, Northeastern University, Boston, Mass., June 1974.
17. A. Ray, and H.F. Bowman,"A Nonlinear Dynamic Model of a Once-through Subcritical Steam Generator," J. Dynamic Systems, Measurements, and Control, Trans. ASME, Vol. 98, Ser. G, No.3, pp.332-339, Sept. 1976.
18. IBM Continuous System Modeling Program III (CSMP III), Se. No. SH19-7001-3, Dec. 1975.
19. T.E. Springer, and O.A. Farmer, "TAF - A Steady-state, Frequency Response and Time Response Simulation Program," Fall Joint Computer Conference, 1968.
20. G. Hastings, and J. Louis, "Control Design Development for a HTGR Plant by Digital Simulation," Proceedings of the 7th PICA, IEEE, pp.463-470, May 1971.
21. D.C. Richardson, "Linear Modeling and Control of the High Temperature Gas-cooled Reactor (HTGR) Power Plant," Summer Computer Simulation Conference, San Diego, Calif., Paper No. IV-4.1, pp. 738-750, June 1972.
22. P. Bogorinski, K. Friedrich, J. Schutz, and H. Vollmer, "Dynamics and Control of the Thorium High Temperature Reactor (THTR) Power Station," Int. Conf. Boiler Dyn. & Contr., U.K., Ch.7, March 1973.
23. R.W. McNamara, M.R. Ringham, C.C. Bramblett, and L.C. Southworth, "Practical Simulation of an Industrial Fluid System with Controls - The Circulator Auxiliaries for the Fort St. Vrain Nuclear Generating Station," Preprints, Joint Automatic Control Conference, pp. 345-350, 1977.
24. M.M. El-Wakil, Nuclear Heat Transport, International Press, 1971.
25. Y. Lin, R.S. Nielsen, and A. Ray, "Fuel Controller Design in a Once-through Subcritical Steam Generator System," Journal of Engineering for Power, Trans. ASME, Vol. 100, No.1, pp. 189-196, Jan. 1978.
26. N.R. Sandell, and M. Athans, Modern Control Theory Computer Manual, Center for Advanced Engineering Study, M.I.T. Press, Cambridge, Mass., 1974.
27. W. Gabler, "Simplified Neutron Kinetics with Known Approximation Error," Proceedings of the American Nuclear Society Winter Meeting, pp. 355-366, Nov./Dec. 1969.
28. R.E. Skinner, and E.R. Cohen, "Reduced Delayed Neutron Group Representation", Nuc. Sci. and Eng., Vol. 5, pp. 291-298, 1959.

APPENDIX I

NUCLEAR REACTOR MODEL

Dynamic equations for prompt neutron and 6 delayed neutron groups were simplified in the model. Since the prompt group is very fast (lifetime in the order of milliseconds), its effects were assumed instantaneous. Reduced (2- and 3-) group models have been shown to be adequate for dynamic representation of delayed neutron characteristics over a wide frequency range.[27,28] Since a 3-group model does not offer a significant improvement over a 2-group model, the 6 delayed group process was approximated by a 2-group model.[28] Total reactivity ρ was obtained as

$$\rho = \rho_c + \rho_f + \rho_m$$

where ρ_c = a function of reactor control rod insertion;
ρ_f = a function of average fuel temperature; and
ρ_m = a function of average moderator temperature.

Core temperature variations in the axial direction were approximated by two identical lumped sections. In the radial direction, fuel and moderator temperatures were treated separately due to widely different temperature coefficients of reactivity. Assumptions in the formulation of core thermal model were: (1) Thermal energy is radially transferred from fuel to helium via graphite moderator; and (2) Thermal properties of enriched UO_2 fuel graphite moderator and helium coolant are constant over the operating range.

APPENDIX II

LIST OF STATE, OUTPUT AND INPUT (CONTROL) VARIABLES

This state-space model has 40 state variables $\underset{\sim}{x}$ 11 output variables $\underset{\sim}{y}$, and 5 input variables $\underset{\sim}{u}$:

State Variables $\underset{\sim}{x}$

Concentration of 1st lumped delayed neutron group;
Concentration of 2nd lumped delayed neutron group;
Average fuel temperature in upper half of reactor core;
Average fuel temperature in lower half of reactor core;
Average moderator temperature in upper half of reactor core;
Average moderator temperature in lower half of reactor core;
Steam pressure, upstream of circulator turbine bypass valve;
Steam pressure at circulator turbine inlet;
Steam density at circulator turbine exhaust;
Specific steam enthalpy at circulator turbine exhaust;
Circulator turbine-compressor shaft speed;
Helium temperature at compressor inlet;
Helium temperature at reactor lower plenum;
Economizer length in main steam generator;
Average specific internal energy of compressed water in economizer;
Average tube wall temperature in economizer at mean radius;
Economizer-evaporator length;
Average tube wall temperature in evaporator at mean radius;
Density of saturated steam at evaporator-superheater boundary;

Average specific internal energy of steam in superheater;
Average tube wall temperature in superheater at mean radius;
Average specific enthalpy of steam in reheat steam generator;
Average tube wall temperature in reheat steam generator at mean radius;
Steam density at main steam generator discharge;
Specific steam enthalpy at main steam generator discharge;
Main (throttle) steam pressure;
Steam pressure downstream of wide open governor valves;
Steam pressure downstream of partially open governor valves;
Steam pressure at high pressure turbine impulse stage;
Steam density at high pressure turbine exhaust;
Specific steam enthalpy at high pressure turbine exhaust;
Steam density at hot reheat header;
Specific steam enthalpy at hot reheat header;
Steam pressure at intermediate pressure turbine extraction;
Steam pressure at low pressure turbine lumped extraction;
Saturated water temperature in the lumped heater shell;
Specific enthalpy of saturated water in deaerator storage tank;
Feedwater pump-turbine shaft speed;
Feedwater flow;
Specific enthalpy of feedwater at main steam generator inlet.

Output Variables $\underset{\sim}{y}$

Feedwater flow;
Feedwater pump-turbine shaft speed;
Main (throttle) steam pressure;
Main (throttle) steam temperature;
Steam pressure at high pressure turbine impulse stage;
Steam pressure upstream of circulator turbine bypass valve;
Steam pressure at helium circulator turbine exhaust;
Circulator turbine-compressor shaft speed;
Hot reheat steam temperature;
Normalized neutron flux;
Electrical power.

Input Variables $\underset{\sim}{u}$

Governor valve area;
Reactor control rod insertion;
Circulator turbine control valve area;
Circulator turbine bypass valve area;
Feed pump turbine control valve area.

Asok Ray received B.E. and M.E. degrees in Electrical Engineering from Calcutta University, India, and Ph.D. in Mechanical Engineering and M.S. in Mathematics from Northeastern University, Boston. He has been involved in dynamic modeling and control system design of fossil and nuclear power plants. His present academic interests include abstract and applied mathematics, and their applications to biological and clinical problems.

Dr. Ray is a Registered Professional Engineer in the Commonwealth of Massachusetts.

H. Frederick Bowman earned a B.S. degree in Mechanical Engineering at Pennsylvania State University, and M.S., Nuclear Engineer, and Ph.D. degrees in Nuclear Engineering at Massachusetts Institute of Technology. A professor at Northeastern University for nine years, he holds concurrent appointments as lecturer in Mechanical Engineering at MIT and is Senior Academic Administrator of the Harvard-MIT Division of Health Sciences and Technology. His teaching and research interests are in the fields of heat transfer, bioheat transfer, thermal property measurements, cryogenics and thermal modeling of nuclear power plants.